Influence of curing on pore properties and strength of alkali activated mortars

MANGAT, Pal <http://orcid.org/0000-0003-1736-8891> and OJEDOKUN, Olalekan <http://orcid.org/0000-0002-9573-4976>

Influence of curing on pore properties and strength of alkali activated mortars

P.S. Mangat and Olalekan O. Ojedokun

Centre for Infrastructure Management, Materials and Engineering Research Institute, Sheffield Hallam University, Sheffield S1 1WB, UK

ABSTRACT

The paper investigates the effect of wet/dry, wet and dry curing on the pore properties and strength of an alkali activated cementitious (AACM) mortar. The pore characteristics were determined from the cumulative and differential pore volume curves obtained by mercury intrusion porosimetry. AACM mortars possess a bimodal pore size distribution while the control PC mortar is unimodal. AACM mortars have a lower porosity, higher capillary pore volume, lower gel pore volume and lower critical and threshold pore diameters than the PC mortar which indicate greater durability potential of AACMs. Wet/dry curing is optimum for AACM mortars while wet curing is optimum for the PC mortar. Shrinkage and retarding admixtures improve the strength and pore structure of the AACMs.

Keywords: Alkali activated cementitious material AACM, gel pores, capillary pores, cumulative pore volume, differential pore volume, Porosity

Notations:

AACM	Alkali activated cementitious materials
PC	Portland cement
GGBS	Ground granulated blast-furnace slag
ITZ	Interfacial transition zone
p	Absolute applied pressure
r	Pore radius
y	Mercury surface tension (= 0.48N/m)
ϕ	Mercury contact angle (= 140^0)

1.0 Introduction

The use of alkali activated cementitious materials (AACM) in place of Portland cement (PC) has been recognized to have great potential in construction applications. There is the need for a viable alternative to PC because of the high carbon footprint generated during its production with a huge energy demand, which is not sustainable in the future. The carbon footprint is significant because of the large volume of Portland cement PC consumed worldwide, which is ranked second after the volume of water [1]. To put this into perspective, for each tonne of cement produced an equivalent tonne of CO_2 is emitted into the atmosphere. This translates to the emission of 400 Kg of CO_2 per 1 m^3 of concrete production [2]. In addition, the cement industry consumes between 12 - 15% of the total industrial energy use [3]. The electric energy consumption for the burning process during cement production is estimated to be 65 kWh/tonne while the thermal energy consumption for cement grinding is 2.72 GJ/tonne [3]. Clearly, there is a dire need for reducing this carbon foot print and energy demand.

Limited knowledge is available in literature on the pore properties of AACMs and geopolymers [4]. However, established knowledge on the pore properties of conventional concrete [5] shows their critical importance in controlling the durability and strength of concrete. The pore properties are equally important for AACMs and other porous ceramic materials. The refinement of concrete pore structure improves its compressive strength, resistance to diffusion of deleterious substances such as chlorides and CO_2, which affect its durability [6]. These deleterious substances which cause corrosion of steel in concrete are transported through the concrete pores by capillary absorption, hydrostatic pressure and diffusion [7]. Diffusion of the ionic elements (Cl^- and Na^+) is mainly through the pores of the cement paste matrix and not through the interface between cement paste and aggregates [8]. The interface between the cement paste and aggregates accounts for up to 50% of the total

volume of pores in hardened concrete but these were found to be discontinuous and isolated from each other, thereby preventing the penetration of harmful elements through them [8].

The little understanding of the pore properties of AACM concrete provided in current literature suggests that the pore size distribution of AACMs is bimodal under all curing conditions [2,4]. The pores of AACMs are separated into two zones (> 1µm and < 0.02µm ranges) unlike a similar grade of PC matrix which is observed to be unimodal ranging between 0.01µm to 0.1µm [2,4]. Literature suggests that the gel pores in AACMs are formed during the polymerization of aluminosilicate gel during curing [9]. The extent of gel pores formed under different curing regimes is not understood. The gel pores are defined to be within the range of 0.005 to 0.01 µm based on PC concrete research [9]. The large capillary pores which are orders of magnitude bigger than gel pores and are within the range of 0.01 µm to 100 µm based on PC concrete research [9]**.** *Yue and Jiaqi* [10] showed an inverse relationship between the volume of gel and capillary pores as hydration progresses in PC concrete. During the hydration process of concrete, the volume of capillary pores decreases while the gel pores increases. This results in a lower cumulative pore volume in time because the comparatively large capillary pores is partially occupied by the binder gel. Ultimately, a denser microstructure evolves as the hydration progresses. The influence of curing on the pore properties of AACMs such as the gel pores, capillary pores, critical and threshold pore diameters are not defined in literature. These aspects of pore properties of AACMs are reported in this paper.

Pore refinement of PC concrete is achieved by high humidity (> 80% R.H) curing which provides prolonged hydration of cement at low or high temperatures [5]. In the case of AACMs, earlier research has shown a need for high temperature curing at 50 - 80^{0}C, such as steam or dry heat, for optimum geopolymerization reaction [2,11]. More recent work uses ambient temperature (20 ± 2^{0}C), which is practical on construction site, for curing AACMs

[12,13]. The optimum levels of relative humidity required for AACM curing are not established. However, results indicate that "dry" curing at low relative humidity (e.g. 60% R.H.) produces high strength for AACMs unlike PC concrete which has maximum strength under wet curing (100% R.H.) [14,15]. This can be beneficial for practical use of AACMs since insitu curing in construction does not provide idealized wet conditions. Practical site conditions represent a balance between, wet, wet/dry and dry conditions by preventing moisture loss at early age while concrete is exposed to ambient conditions of wetting and drying in the longer term. The practical curing conditions wet/dry, dry and wet at ambient temperature applicable in the field, were adopted in this investigation to determine the benefits of early age moisture available for curing on the strength and pore properties of AACMs.

A potassium-based activator used in AACMs reduces the mean pore diameter more than a sodium-based activator [4] while the total porosity of an alkali activated blast furnace slag (BFS) is reduced by the inclusion of a high modulus (more concentrated) activator and low water content in the mix [2]. The influence of chemical admixtures such as retarder and shrinkage reducing admixtures on the pore properties of AACMs is not known. This aspect together with the influence of activator dilution on the pore properties of AACM mortar is investigated.

Mercury intrusion porosimetry (MIP) is the common test method for investigating the microstructure of concrete. This is performed by applying mercury under high pressure through concrete pores. The method is based on the "non-wetting" property of mercury on the walls of the concrete pores. Mercury intrusion into the concrete matrix is suitable for pores within the range of 0.003 to 400 μm [16]. This method is used for analysing the accessible pores within the AACM and the control PC mortar samples in this investigation.

This paper is part of a comprehensive durability investigation of AACMs (mortar and concrete) being undertaken by the authors. It characterises the basic pore-properties of the material to provide a deeper understanding of the durability properties of reinforced AACM concrete.

2.0 Experimental programme

2.1 Materials and mixes

The control PC mortar had a composition of 1: 2.1 (by weight) of CEM 1 cement to CEN standard sand with a water/cement ratio of 0.47. The CEM 1 cement used is 42.5 Portland cement and it was supplied by Frank Key group, Sheffield, UK. The PC mortar was produced in accordance with BS EN 196-1:2016 [17]. The corresponding AACM 1 and 2 mortar mixes comprised of GGBS binder, sodium silicate and hydroxide based activator, fine aggregate of 80% particle size passing 1mm sieve, liquid/binder ratio of 0.47 (alkali activator + water), a shrinkage reducing admixture SRA and retarder R42. The fresh AACM 1 and 2 mortar mixes were designed to achieve a flow of about 15 cm using the flow table test method [18]. The shrinkage reducing admixture SRA was added to reduce the shrinkage of AACMs while retarder R42 was added to increase the setting time. AACM 1 and 2 mixes were investigated to provide optimum properties of the fresh and hardened material for practical applications. However, AACM 1a and 2a mixes were also prepared with the same mix proportions but without admixtures to provide data for direct comparison with the PC mix which also did not contain admixtures. The mix compositions for AACM 1, 2, 1a, 2a and the control PC mortars are presented in Table 1. Table 2 shows the chemical composition of Portland cement (PC) and ground granulated blast-furnace slag (GGBS) binders used in the tests.

The average 28-day strength of the AACM and control PC mixes were designed to be fairly similar under wet curing, based on trial mixes. Wet curing is the standard method for quality

148 testing of concrete [5]. The different curing methods adopted in this research are detailed in
149 section 2.2.

150 Table 1: Composition of the AACM and control PC mortars

Mix	Binder (%)	Fine Agg. (%)	Liquid (%)	Liquid/Binder Ratio	Activator Dilution (%)	R42 (% binder)	SRA (% binder)
AACM 1	49	28.0	23.0	0.47	0	0.75	2.0
AACM 2	49	28.0	23.0	0.47	7.76	0.75	2.0
AACM 1a	49	28.0	23.0	0.47	0	-	-
AACM 2a	49	28.0	23.0	0.47	7.76	-	-
Control PC	28	59.0	13.0	0.47	-	-	-

151 Table 2: Chemical composition of Portland cement and GGBS binders

Chemical component	SiO_2	Al_2O_3	Fe_2O_3	CaO	MgO	K_2O	Na_2O	TiO_2	P_2O_5	MnO	SO_3
PC (mass %)	11.1	8.35	3.16	64.2	2.09	1.19	0.227	1.88	2.01	2.14	3.64
GGBS (mass %)	28.6	12.4	5.7	42.3	6.1	0.8	0.4	1.78	<0.1	0.3	0.08

152 Sodium silicate activator of molarity 6.5 mol/L and modulus 2% was used for the AACM
153 mixes to provide optimum viscosity for controlling workability and setting time [19]. The
154 molarity of NaOH activator used was 4.8 mol/L. The combined molarity of the activators was
155 at the lower end of values used by other researchers [20] for a similar activator combination.
156 The activator for AACM 2 mixes was diluted with water at 7.76% (Table 1). The retarder
157 R42 is made from a blend of high grade Polyhydroxycarboxylic acid derivatives while the
158 shrinkage reducing admixtures (SRA) is made from Alkyl-ether. Each admixture contained
159 less than 0.1% chloride ion and 3.5% sodium oxide.

160 *2.2 Casting and curing*

161 The GGBS binder and saturated surface dry fine aggregate were placed in a 12 litre, 3 speed
162 Hobart mixer. They were mixed for 30 seconds at the lowest speed (option-1) to avoid
163 dispersing the powder into the atmosphere. The liquid component containing the activator
164 and retarder R42 were slowly added to the mix. Mixing continued for 2 minutes until a

uniform texture was produced. The shrinkage reducing admixture SRA was then slowly added while mixing continued. The mortar was further mixed for 1 minute before stopping. The control PC mortar and the AACM mixes without admixtures were prepared in a similar manner without adding retarder R42 and shrinkage reducing admixture SRA. The AACM and control PC mortars were cast in 75 x 75 x 75 mm steel cube moulds which had been lightly oiled to prevent the hardened mortar from sticking to the surface. Three mortar cubes were cast for each mix. The specimens were left covered in the moulds with polythene sheets for 24 hours at room temperature of 20 ± 2 ^{0}C and a relative humidity of about 65%. The specimens were demoulded 24 hrs after casting and were exposed to three different curing regimes.

Three practical curing regimes (wet/dry, wet and dry), commonly applied in the construction field, were adopted in this research work as shown in Table 3. Wet/dry curing involved placing the mortar cubes in water at a temperature of 20 ± 2^{0}C for 3 days immediately after demoulding (24 hrs after casting), followed by dry curing in the laboratory air at a temperature of 20 ± 2^{0}C and approximately 65% relative humidity for 24 days (total curing period of 28 days). Wet curing was provided by placing the cube specimens in water at a temperature of 20 ± 2 ^{0}C for 27 days immediately after demoulding. Dry curing of the mortars was provided by exposing them in the laboratory air at a temperature of 20 ± 2^{0}C and approximately 65% relative humidity for 27 days after demoulding. When cured in the laboratory air (during wet/dry and dry curing), the specimens were securely covered with polyethene sheets to prevent moisture loss from the concrete surface representing site practice where different methods can be used to prevent rapid drying of concrete such as applying curing membranes or covering concrete surface with wet hessian.

Table 3: Curing methods used for the AACM and control PC mortars

Samples	Age(days)	Wet/dry	Wet	Dry

		(Curing Medium)	(Curing Medium)	(Curing Medium)
75 mm cubes	0-3	Water	Water	Air
	3-28	Air	Water	Air
MIP samples	28-31	Oven (50^0C)	Oven (50^0C)	Oven (50^0C)
	31-34	Desiccator	Desiccator	Desiccator

2.3 Test procedure

2.3.1 Compressive strength

The compressive strength and density of the 75 mm mortar cubes were determined after 28 days curing under wet/dry, wet and dry regimes (Table 3). The compressive strength tests on the cubes were conducted in accordance with *BS EN 12390-3:2009* [21]. The density of the cubes was determined according to *BS EN 12390-7:2009* [22]. Three specimens were used to determine the density and compressive strength of the 75 mm cubes. A loading rate of 3 MPa/min was applied during the compression testing and a post peak of 30% failure load was programmed into the compression machine to prevent complete disintegration of the crushed specimen. Samples for the Mercury intrusion porosimetry (MIP) tests were obtained from these crushed samples.

2.3.2 Mercury Intrusion Porosimetry

Mercury intrusion porosimetry (MIP) test samples, with a weight of 1 - 2 g and average length of 1 cm, were obtained from the crushed 75 mm mortar cubes. Errors caused by hysteresis and entrapment of moisture during MIP testing was minimised by controlling the dimensions, mass and drying of all test samples [23] as described here. The mercury intrusion porosimetry (MIP) test samples were dried in an oven at a temperature of 50^0C for 3 days (28- 31 days age) as shown in Table 3. Oven drying at a higher temperature than 50^0C causes microcracking which may adversely affect the test results [24]. After oven drying for 3 days,

the samples were placed in a desiccator for another 3 days to reduce their temperature to about 20^0C. The desiccator had silica gel at the bottom to further assist with removing absorbed water and preventing moisture migration from the air. The drying and cooling were carried out to remove absorbed water within the mortar pore system, which can obstruct its accessible porosity during MIP testing.

MIP testing was performed using a Pascal 140/240 Porosimeter which is in two parts. Pascal 140 applies pressure of up to 100 MPa and Pascal 240 applies pressure of up to 200 MPa to aid the intrusion of mercury through pore sizes down to 0.007 µm. The Pascal 140/240 Porosimeter measures pore sizes within the range of 0.007 to 100 µm. Its computer microprocessor translates the data collected on the applied pressures to pore radius using the Washburn equation (equation 1).

$$p = \frac{2y\cos\phi}{r} \qquad 1$$

Where p is the absolute applied pressure; r is the pore radius; y is the mercury surface tension (= 0.48N/m); ϕ is the contact angle (= 140^0).

The limitation of Washburn equation is the assumption that the pores in the concrete matrix are cylindrical in shape which has been criticised by researchers [23]. The graphs of pore sizes and pore distribution were obtained at the end of the mercury intrusion porosimetry analysis. The MIP analysis was performed on three test samples for each curing condition for the AACM and control PC mortars.

3.0 Results and discussion

3.1 Compressive strength and density

The average value of the compressive strength and density of the three specimens tested per mix had less than 5% variation.

3.1.1 Effect of curing regimes on density and compressive strength

The densities of the 75 mm mortar cubes at 28 days age are between 2.22 - 2.35 g/cm^3 for wet/dry curing, 2.10 - 2.23 g/cm^3 for dry curing and 2.07 - 2.15 g/cm^3 for wet curing. The corresponding 28day compressive strength for the AACM and control PC mortars under wet/dry, wet and dry curing (Table 3) are shown in Fig. 1.

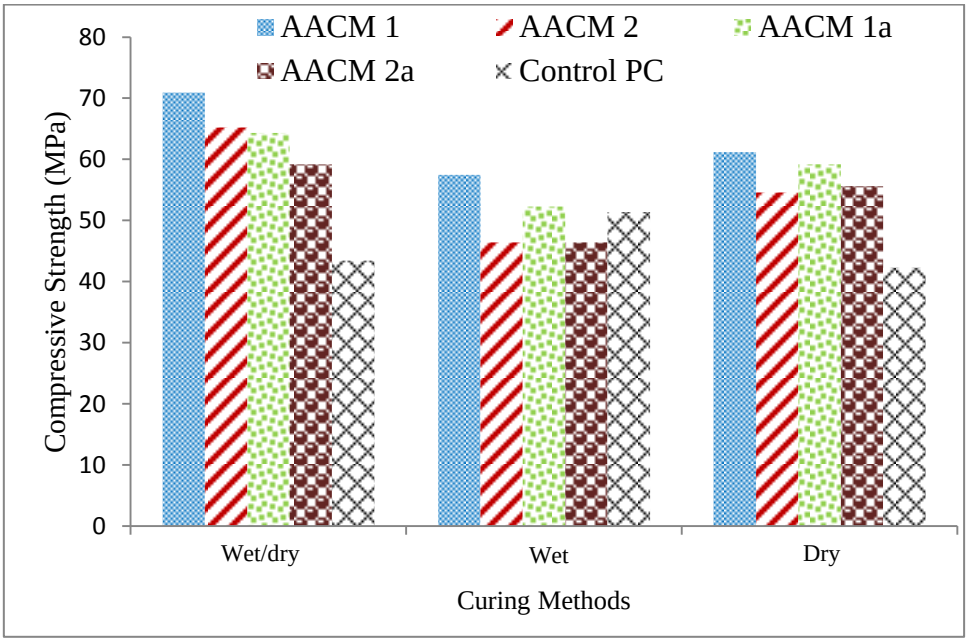

Fig. 1: Compressive strength of AACM and control PC mortars under wet/dry, wet and dry curing at 28 days

The compressive strengths of AACM 1 are 70.9 MPa for wet/dry curing, 57.9 MPa for wet curing, and 61.2 MPa for dry curing. The corresponding values for AACM 2 are 65.2 MPa, 46.4 MPa and 54.6 MPa. Similar trend is observed in AACM 1a and 2a. The wet/dry curing method achieved the highest strength for all the AACM mortars. This curing method involved 3 days wet curing at 20 ± 2^{0}C followed by 24 days in the laboratory air (20 ± 2^{0}C, 65% R.H.). The dry curing method of AACM 1 and 2 mortars (27 days curing in laboratory air at 20 ± 2^{0}C, 65% R.H.) gave lower strength than the wet/dry method while wet curing (27 days curing in water at 20 ± 2^{0}C) gave the least compressive strength. The wet/dry curing of AACM mixes gave the highest strength due to the formation of more crystalline geopolymerisation products [2,11].

The effect of curing methods on the control PC mortar contrasts the AACM mortars by providing the maximum compressive strength under wet curing. The availability of moisture in the PC mortar supported cement hydration which produced more strength. The geopolymer reactions in AACMs do not rely on moisture to the same extent as the hydration reactions in PC. The control PC mortar recorded the highest compressive strength of 51.4 MPa (Fig. 1) under wet curing followed by 43.4 MPa under wet/dry curing, which is slightly higher than 42.3 MPa under dry curing as shown in Fig. 1. The results of the control PC mortar are consistent with other research which shows a similar effect of curing conditions on the strength of PC concrete [25,26]. The relative humidity in the PC capillary pores is maintained above 80% when cured in water, which favours hydration reactions [5]. There is little loss of strength when PC concrete is cured in a moist medium above 80% R.H.

The 28 day strengths of AACM 1, 2 (both with retarder and shrinkage reducing admixture) and PC mortar (without the admixture) under wet curing are 57.4 MPa, 52.3MPa and 51.4MPa respectively. The compressive strengths under wet curing of AACM mortars 1a and 2a (both without admixture) average 46.4 MPa and 46.2MPa respectively compared with 51.4MPa for wet cured PC mortar. The average strength of the AACM mixes is similar to the PC mortar (control) mix under wet curing whereas their strength is much higher under partially dry curing conditions (wet/dry and dry) which are encountered on site.

3.1.2 Effect of activator dilution on compressive strength

Fig. 1 shows the effect of activator dilution on the compressive strength of the AACM mortars under wet/dry, wet and dry curing. The compressive strength decreases with increasing dilution of activator. For example, the compressive strengths of AACM 1 mortar were 70.9 MPa, 57.9 MPa and 61.2 MPa compared with 65.2 MPa, 46.4 MPa and 54.6 MPa for AACM 2 mortar (7.76% dilution) under wet/dry, wet and dry curing respectively (Fig. 1).

Activator concentration is an effective factor in the geopolymerisation process in AACM concrete. A reduction in strength has been reported when the activator concentration is not sufficient for the geopolymerisation reaction [11,27]. Similarly, high activator concentration will delay the AACM formations due to excessive cations, thereby limiting their mobility and potential to interact with the reactive pozzolanic species [27]. This reverse effect of strength reduction with increasing concentration of the alkali activator was, however, not observed in this study.

3.2 Pore size distribution

3.2.1 Unimodal and bimodal pore distribution

The relationship between pore size and differential pore volume for AACM 1, 2 and the control PC concrete under wet/dry, wet and dry curing are shown in Figures 2, 3 and 4 respectively.

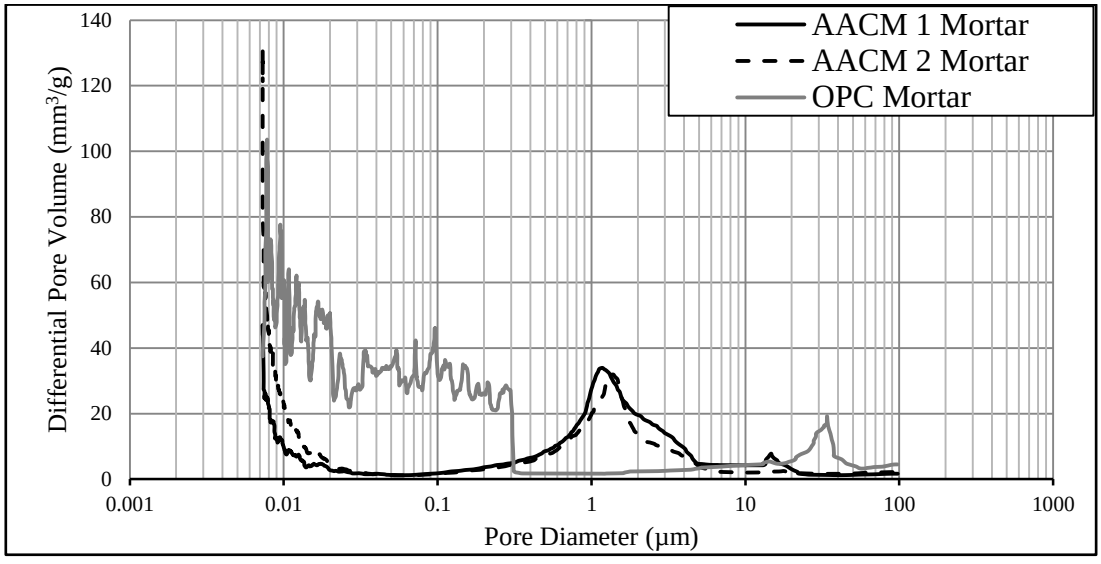

Fig. 2: Pore size distribution for AACM 1, 2 and control OPC mortars under wet/dry curing

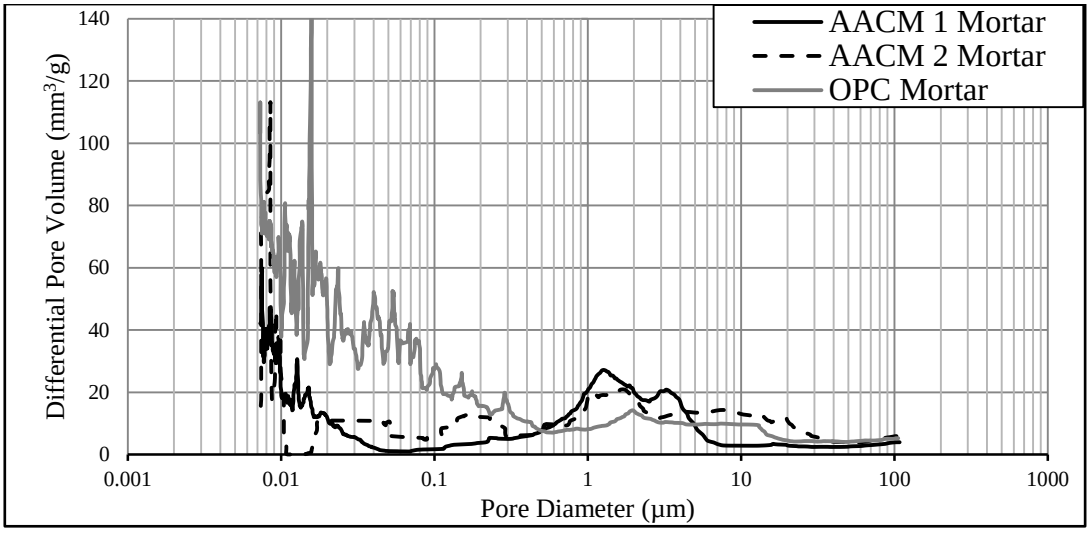

286

287 Fig. 3: Pore size distribution for AACM 1, 2 and control OPC mortars under wet curing

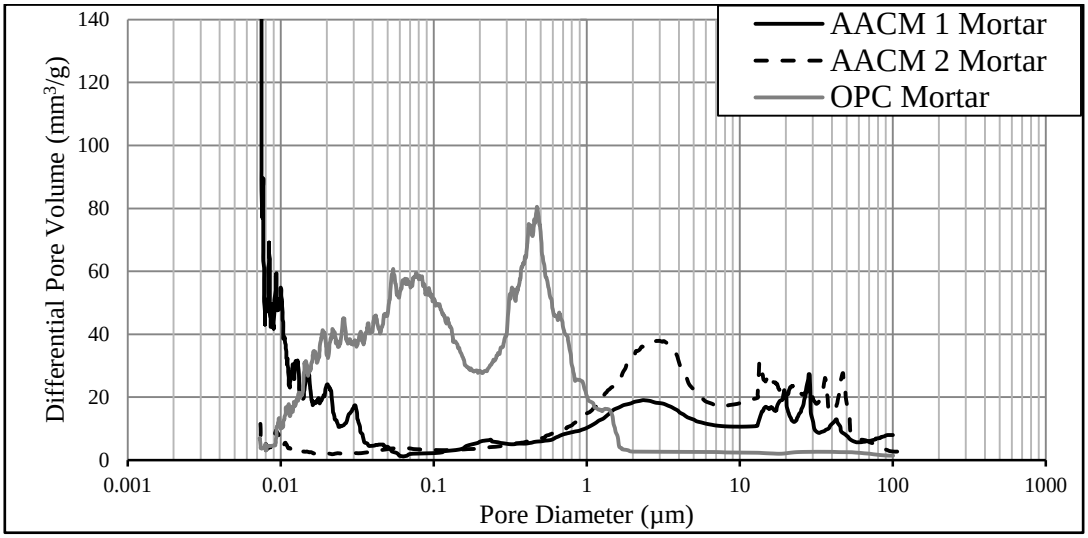

288

289 Fig. 4: Pore size distribution for AACM 1, 2 and control OPC mortars under dry curing

290 The figures show the range of pore diameters under which significant levels of differential
291 pore volumes are observed and the range when the differential pore volume is at or near zero.
292 The diameter zones showing significant differential pore volume represent porosity whereas
293 the range indicating zero differential pore volume represents a non-porous zone. Based on
294 these criteria, it can be observed that the PC mortar has a unimodal pore distribution under
295 the three curing conditions shown in Figures 2, 3 and 4. The pore distribution is referred to as
296 unimodal when a single range of pore volume is observed within the differential pore volume
297 graphs [2,4]. The pore volume of the PC mortar falls within the range of 0.01 to 0.1 µm pore

298 diameter. Other studies on the microstructure of PC matrix also show a unimodal pore size
299 distribution with most of the pore volume within the range of 0.01 to 0.1 μm pore diameter
300 [2,4]. On the other hand, a double range of pore diameters with significant differential pore
301 volume which are separated by a diameter range with nearly zero differential pore volume is
302 categorized as a bimodal pore distribution [2,4]. These pore sizes are normally observed
303 between two separate zones of > 1 μm and <0.02 μm [2]. Figures 2, 3 and 4 show that
304 AACM 1 and 2 mortars fall under this category with significant porosity observed at > 1 μm
305 and <0.02 μm while there is little porosity between these pore size ranges.
306 The differences in the effects of wet/dry, wet and dry curing on the differential pore volumes
307 over the pore diameter ranges in Figures 2, 3 and 4 have been quantified by determining the
308 pore system parameters such as porosity and are discussed fully in section 3.3.
309 *Wet/dry curing*
310 The pore sizes in AACM 1 and 2 mortars subjected to wet/dry curing (Fig. 2) show a bimodal
311 pore size distribution. The first range of pore diameters showing significant differential pore
312 volumes in AACM 1 mortar is <0.02 μm while the second range is predominantly between
313 0.2 to 4.5 μm. There is insignificant differential pore volume between 0.02 and 0.2 μm
314 diameter. AACM 2 mortar shows a similar trend of bimodal pore distribution, the pore
315 diameters range from under 0.03 μm to greater than 0.2μm. On the other hand, the control PC
316 mortar shows a unimodal pore size distribution (Fig. 2) of diameter lesser than 0.3 μm. The
317 bimodal distribution of pores in AACM 1 and 2 mortars extends to larger pore diameters than
318 the control PC mortar; however the large pore size zone is isolated due to the bimodal
319 distribution, which will affect porosity as discussed in section 3.3.
320 *Wet curing*
321 The bimodal pore size distribution in AACM 2 mortar is less pronounced under wet curing
322 (Fig. 3) than under wet/dry (Fig. 2) or dry curing (Fig. 4). There is significant continuity of

pores between pore diameters 0.01 to 100 μm (particularly AACM 2) which is reflected by the differential pore volume remaining slightly above zero in this pore diameter range. This does not appear under both wet/dry and dry curing. Therefore some interconnection between the gel pores (< 0.05 μm) and capillary pores (0.1 to 100 μm) is likely in wet cured AACM 2 mortar. The interconnection is represented by the regular distribution of peaks throughout the range of pore sizes 0.01 to 100 μm (particularly AACM 2). The less solid gel products produced in AACM 2 mortar due to the higher activator dilution may be insufficient to block the interconnecting pores. Another reason for pore continuity could be the leaching of alkali cations into the curing solution thereby resulting in loss of alkali concentration needed for geopolymerisation reaction [28]. A slight degree of hydration reactions may also be a likely contributor to the interconnection of pores under wet curing in the AACM 2 due to the high degree of moist curing.

Dry curing

AACM 1 and 2 mortars under dry curing (Fig. 4) show a bimodal pore size distribution similar to wet/dry curing. The first range of pores in AACM 1 mortar are less than 0.05 μm while the second range of the bimodal pore size distribution is greater than 0.1 μm and extends to 100 μm diameter. AACM 2 mortar has slightly different pore ranges of less than 0.02 μm and greater than 0.1 μm and extends to 100 μm diameter. The control PC mortar has a unimodal pore distribution between 0.01 μm to approximately 2 μm, the pore diameter range is higher than under wet/dry and wet curing. The PC mortar shows significant differential pore volume within the dip between the two peaks in Figure 4, unlike the AACMs where the differential pore volume reaches near zero between the bimodal peaks.

3.3 Pore system parameters

Pore system parameters are frequently used in analytical and empirical property-microstructure relationship models [29,30]. These parameters are derived from the

cumulative porosity curves and logarithmic differential pore volume curves. They are classified as intrudable porosity Φ_{in}, critical pore diameter d_c, threshold pore diameter d_{th} and porosity [29,30]. The location of Φ_{in} is shown on the cumulative pore volume curve for both PC and AACM mortars (Figures 5 and 6). The location of d_c and d_{th} is shown on the corresponding differential pore volume curves in these figures. Two locations of d_c and d_{th} are given on the bimodal graphs of AACM mortars. The porosity of cementitious material is the percentage of pores in the total bulk volume of the mortar whereas intrudable porosity represents only the pore volumes which are accesible to mecury intrusion [29]. The values of these pore parameters are presented in Table 4. The porosity and pore volumes of AACM and control PC mortars with and without shrinkage reducing admixture SRA and retarder R42 are presented in Table 4.

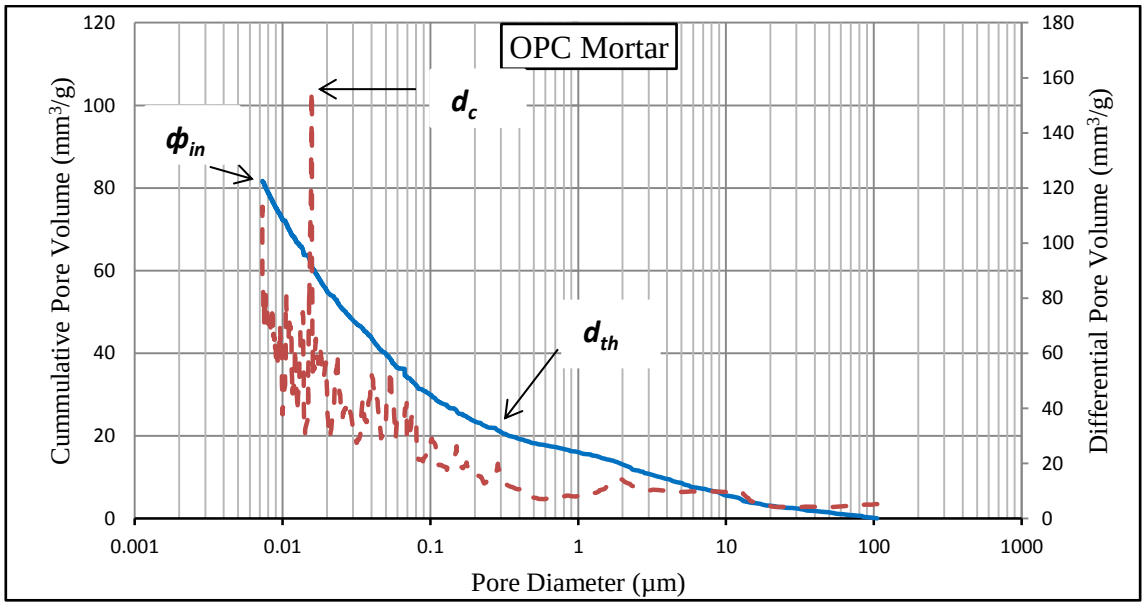

Fig. 5: Definition of Pore System Parameters in OPC Mortar (Authors' data)

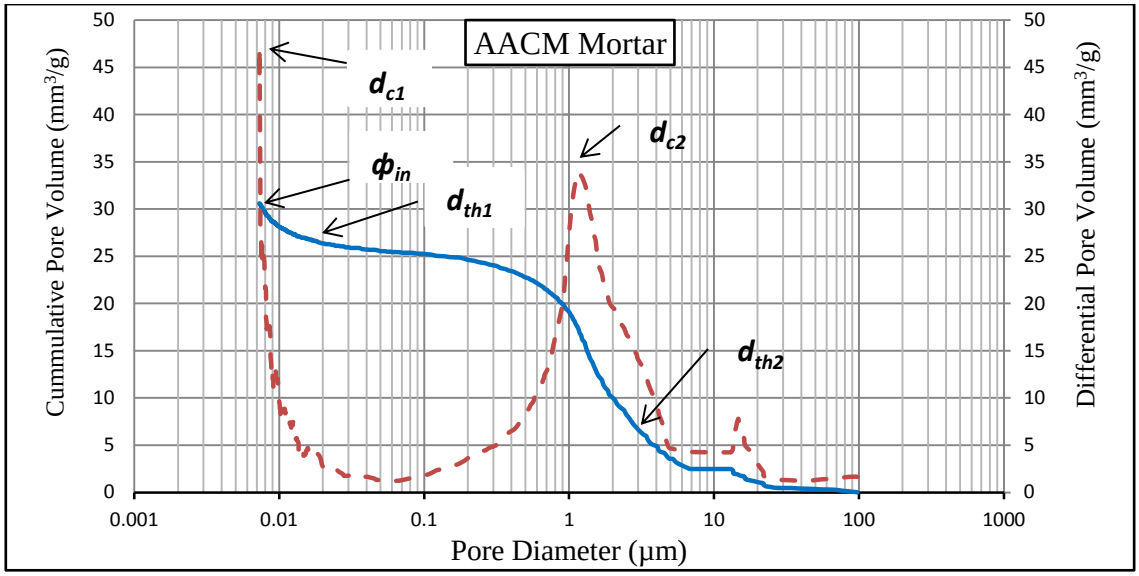

Fig. 6: Definition of Pore System Parameters in AACM Mortar (Authors' data)

Table 4: Pore system parameters for AACM and the control PC mortars

	Mix	Curing	Porosity		Pore diameters (µm)		Pore volumes (%)	
			Intrudable (mm^3/g)	Porosity (%)	Critical d_{c1}	Threshold d_{th1}	Gel	Capillary
With admixtures	AACM 1	Wet/dry	29.68	4.64	0.0073	0.013	0.60	4.04
		wet	38.14	6.53	0.0073	0.014	0.66	5.87
		dry	53.44	9.90	0.0075	0.025	1.42	8.48
	AACM 2	Wet/dry	30.17	6.67	0.0073	0.021	0.98	5.69
		wet	45.48	8.02	0.0081	0.034	0.91	7.11
		dry	59.13	10.70	0.0085	0.048	1.65	9.05
Without admixtures	AACM 1a	Wet/dry	44.26	7.71	0.0081	0.018	0.26	7.45
		wet	51.66	9.05	0.0082	0.019	0.97	8.08
		dry	65.64	11.93	0.0084	0.032	1.92	10.01
	AACM 2a	Wet/dry	46.92	9.14	0.0086	0.027	1.18	7.96
		wet	53.83	10.13	0.0087	0.032	1.80	8.33
		dry	68.05	11.69	0.0089	0.051	1.96	9.73
	Control PC	Wet/dry	81.62	14.02	0.049	0.35	10.83	3.19
		wet	68.16	13.30	0.016	0.28	8.6	4.70
		dry	93.51	17.43	1.07	1.12	10.58	6.85

3.3.1 Intrudable pore volume

The volume of intrudable pores (intrudable pore volume) within AACM 1, 2 and the control PC mortar matrix was determined under wet/dry, wet and dry curing from the cumulative

367 pore volume curves as shown in Figures 7, 8 and 9 respectively. Figure 10 shows the
368 intrudable pore volume.

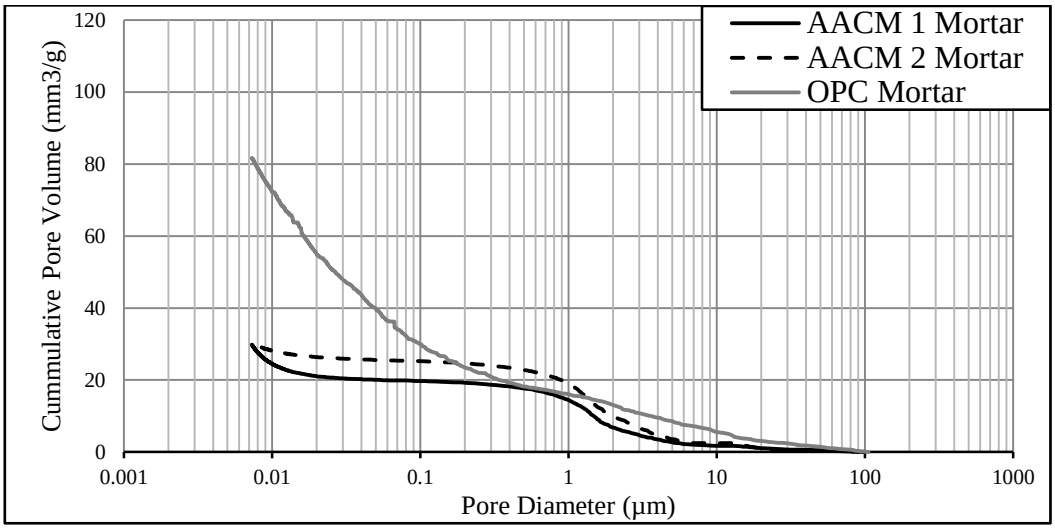

369

370 Fig. 7: Intrudable porosity for AACM 1, 2 and control OPC mortars under wet/dry curing

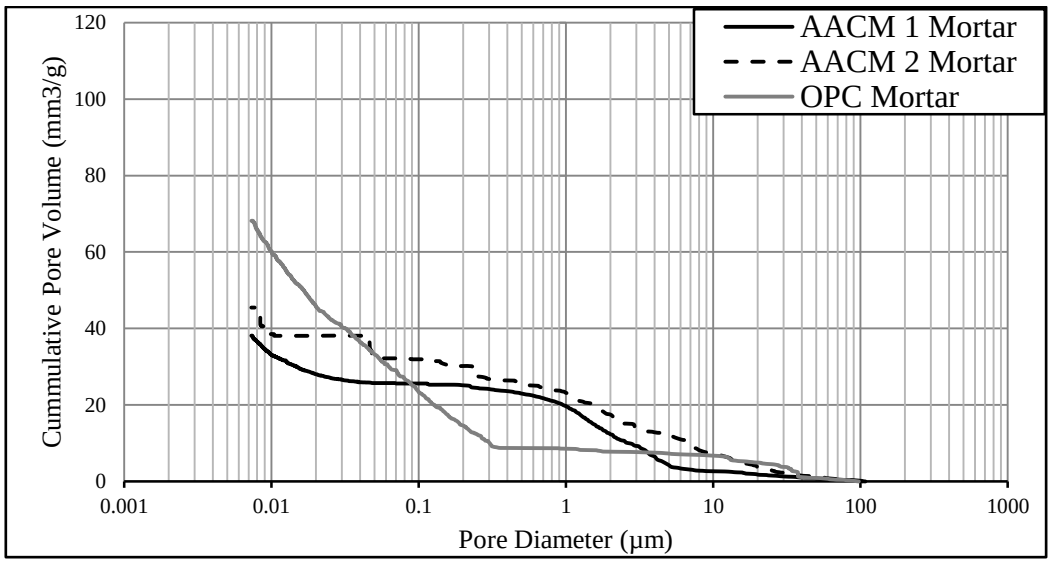

371

372 Fig. 8: Intrudable porosity for AACM 1, 2 and control OPC mortars under wet curing

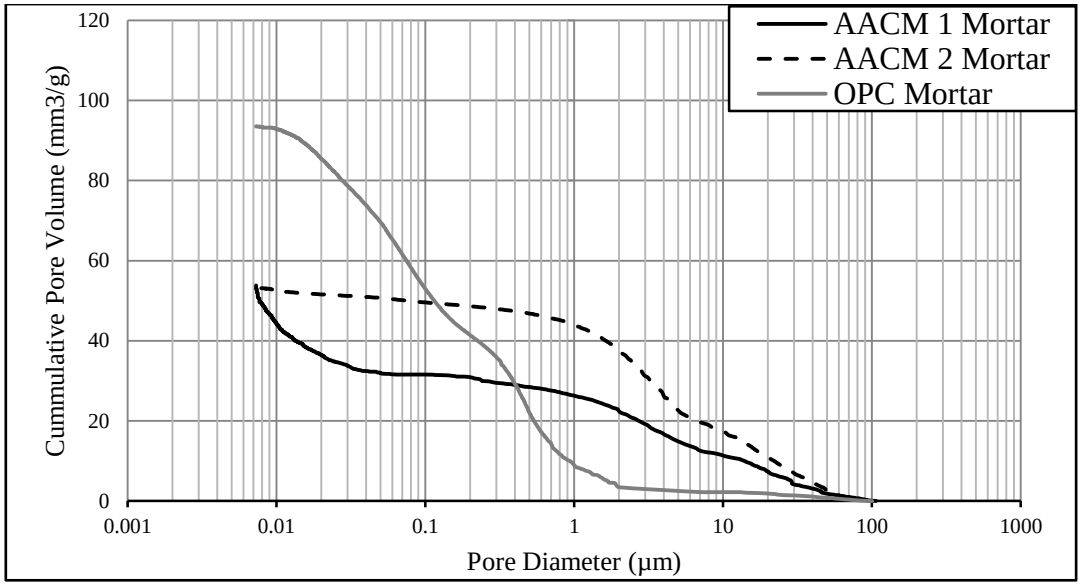

373

374 Fig. 9: Intrudable porosity for AACM 1, 2 and control OPC mortars under dry curing

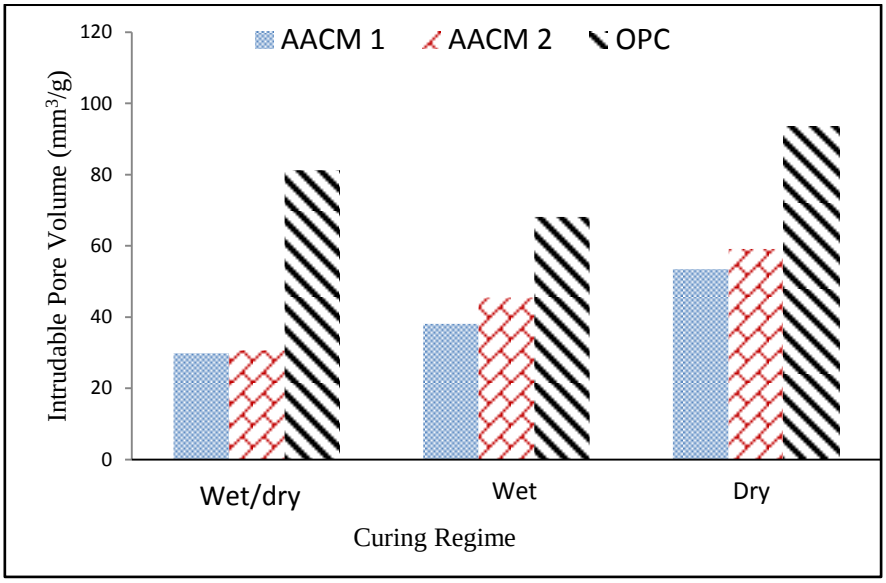

375

376 Fig.10: Intrudable pore volume for AACM 1, 2 and OPC mortars under wet/dry, wet and
377 dry curing

378 *Wet/dry curing*

379 AACM 1 and 2 mortars have lower intrudable pore volume of 29.68 mm^3/g and 30.17 mm^3/g
380 respectively compared with 81.62 mm^3/g for the control PC mortar as shown in Figures 7 and
381 10. The application of wet/dry curing to AACM concrete was observed to enhance its
382 resistance to chloride ingress under exposure to salt laden environment [15]. The initial 3

383 days wet curing followed by the 24 days dry curing in laboratory air under the wet/dry curing
384 method (Table 3) resulted in a lower intrudable pore volume in AACMs.
385 The intrudable pore volume for AACM 1 mortar is similar to the AACM 2 mortar (7.76%
386 activator dilution) at 29.68 mm^3/g and 30.17 mm^3/g respectively under wet/dry curing as
387 shown in Figures 7 and 10.
388 *Wet curing*
389 The wet curing of the control PC mortar resulted in an intrudable pore volume of 68.16
390 mm^3/g (Figures 8 and 10) compared with 81.62 mm^3/g and 93.51 mm^3/g for wet/dry and dry
391 curing respectively (Figures 7 and 9). The wet curing method usually provides the best
392 mechanical and durability properties for PC concrete due to saturation of its pore spaces with
393 water which aid cement hydration. *Powers* [31] and *Patel et al* [32] observed that the
394 hydration of PC concrete is greatly reduced when the relative humidity within the pore spaces
395 drops below 80%. Since both the wet/dry and dry curing methods exposed the control PC
396 mortar to laboratory air (R.H. 65%) before cement paste hydration was completed, it resulted
397 in more intrudable pores than under wet curing.
398 The intrudable pore volume of AACM 1 mortar (38.14 mm^3/g) under wet curing (Fig. 8) is
399 more than (29.68 mm^3/g) under wet/dry curing (Fig. 7). AACM 2 mortar also shows a
400 similarly higher intrudable pore volume under wet curing (Fig. 8).
401 *Dry Curing*
402 AACM 1 mortar has an intrudable porosity of 53.44 mm^3/g compared with 93.51 mm^3/g for
403 the control PC mortar under dry curing (Figures 9 and 10). The results presented in Figures 7,
404 8, 9 and 10 indicate that AACM 1 and 2 mortars possess significantly less intruded pore
405 volume than the control PC mortar under the three curing conditions.
406 *3.3.2 Critical and threshold pore diameters*

The critical and threshold pore diameters of a concrete matrix influence its durability properties [29,30,33]. Lower values of these parameters represent enhanced durability properties. AACM mortars under wet/dry curing had the lowest critical and threshold pore diameters, followed by wet and dry curing. For example, AACM 1 had critical pore diameter of 0.0073 µm both under wet/dry and wet curing and 0.0075 µm under dry curing (Table 4). The corresponding threshold pore diameter was 0.013 µm, 0.014 µm and 0.025 µm. The higher dilution of alkali activator in AACM 2 increased the critical and threshold pore diameters as shown in Table 4. This pattern is similar for the three curing regimes wet/dry, wet and dry. The difference in values under the three curing conditions is more pronounced for the AACM 2 mix than AACM 1.

On the other hand, PC mortar under wet curing has the lowest critical and threshold pore diameters compared with wet/dry and dry curing. The critical pore diamters are 0.016 µm, 0.049 µm and 1.07 µm under wet, wet/dry and dry curing respectively. The corresponding threshold pore diameters are 0.28 µm, 0.35 µm and 1.12 µm in Table 4. The pore blocking effect in PC concrete was proposed by *Khatib and Mangat* [34] for the wet curing regime. The availability of water during curing allowed for more hydration to take place resulting in the formation of more calcium silicate gel thereby reducing the critical and threshold pores.

AACM mortars displayed lower critical and threshold pore diameters than PC concrete. Therefore, the durability properties of AACM mortars are expected to be superior to the PC mortar. Early results from a comprehensive durability study by the authors indicate that chloride diffusion in the PC mortar is greater than the AACM mixes [15]. The relationship between chloride diffusion and the critical and threshold diameters will be addressed in a future paper by the authors.

3.3.3 *Porosity of AACM and PC mortar*

The relationship between porosity and incremental pore diameter range of AACM 1 and the control PC mortars under wet/dry, wet and dry curing are shown in Figures 11, 12 and 13 respectively.

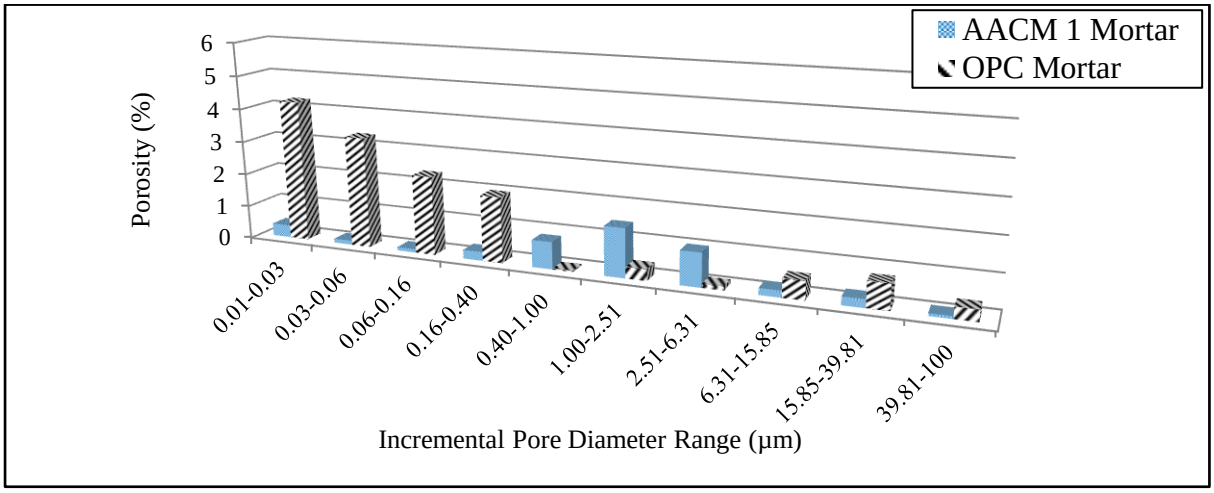

Figure 11: Relationship between porosity and incremental pore diameter (µm) range for AACM 1 and control OPC mortars under wet/dry curing.

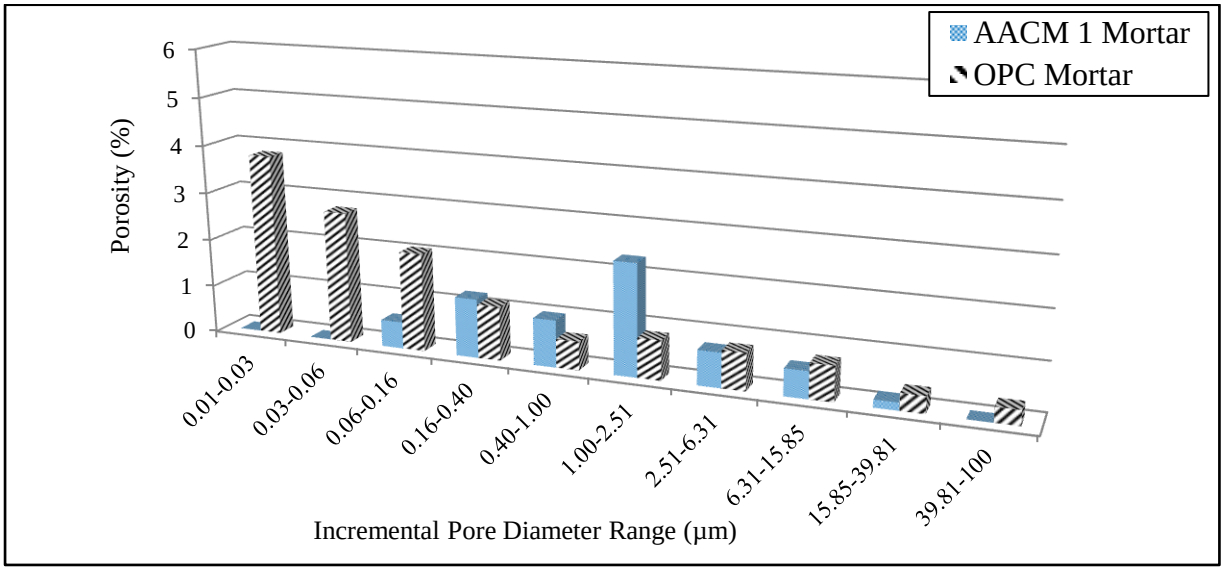

Figure 12: Relationship between porosity and incremental pore diameter (µm) range for AACM 1 and control OPC mortars under wet curing.

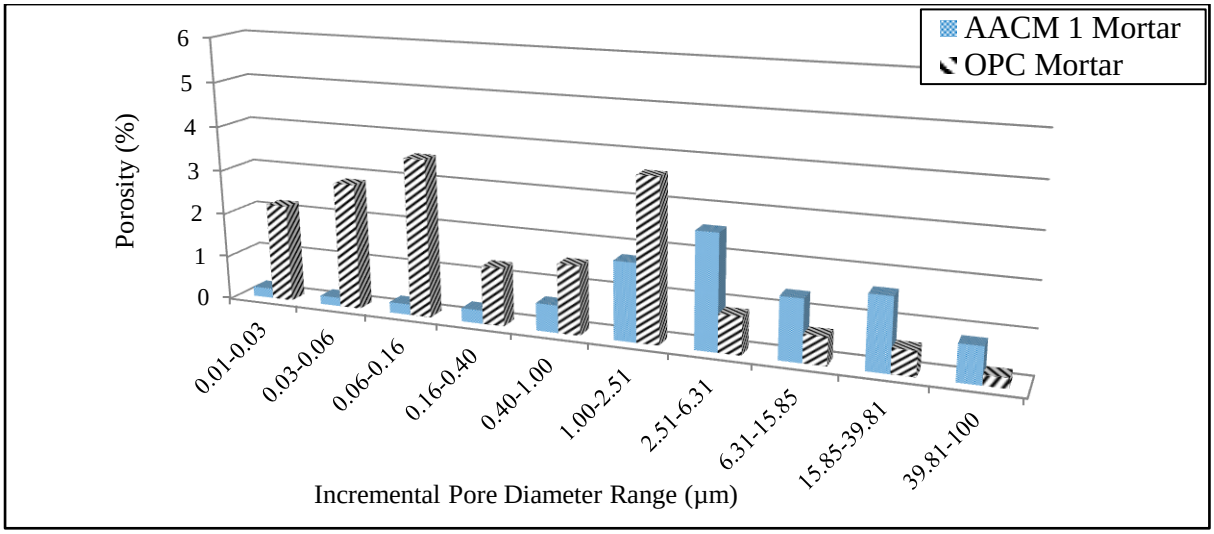

Figure 13: Relationship between porosity and incremental pore diameter (µm) range for AACM 1 and control OPC mortars under dry curing.

The figures show that the porosity of AACM 1 mortar is distributed along a limited range of pore diameters with more significant porosity at larger diameters. On the other hand, the control PC mortar has its porosity distributed along the whole range of pore diameters with more significant porosity at smaller diameters. The AACM mortars show a distinctively large volume of pores within the capillary pore zone (>0.16 µm) while PC mortars have a large volume of pores within the gel pore zone (<0.16 µm). For example, the percentage of capillary pore volume is 4.04% and 3.19% for AACM 1 and PC mortars respectively under wet/dry curing. The corresponding gel pore volume is 0.60% and 10.83%

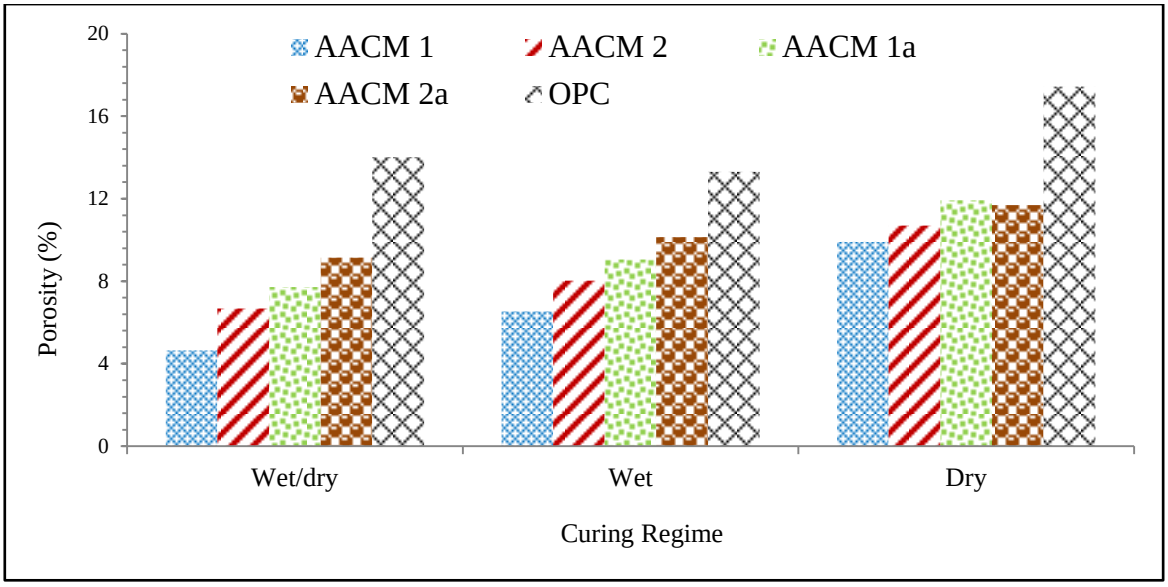

Figure 14: Effective porosity of AACM and control OPC mortars under wet/dry, wet and dry curing.

Fig. 14 shows the effective porosity of AACM 1 and the control PC mortars under wet/dry, wet and dry curing. This is the summation of the incremental pore volumes in Figures 11, 12 and 13. The porosity of AACM 1 mortar is much lower than the control PC mortar despite the presence of larger pores in AACM 1 mortar. The porosity of AACM 1 mortar is 4.64%, 6.53% and 9.90% compared with 14.02%, 13.30% and 17.43% for the control PC mortar under wet/dry, wet and dry curing respectively. The porosity for the corresponding AACM 2 mortar is 6.67%, 8.02% and 10.70%.

The porosity of AACM mix 1a is 7.71%, 9.05% and 11.93% for wet/dry, wet and dry curing respectively. Each value is significantly lower than the corresponding value for PC mortar. AACM mix 1a did not incorporate any admixtures (SRA and R42) and, therefore, is directly comparable with the PC mortar. The porosity of AACM mix 2a is similarly lower than the PC mortar. The results confirm the lower porosity of the AACM mixes.

The wet/dry curing is optimum for AACM mortar while wet curing is best for the control PC mortar, the latter being a well-established fact.

RILEM TC 224 [2] reported that the total porosity (i.e. summation of both gel and capillary pores) of AACM is somewhat similar or sometimes higher than comparative PC. The contrary results of this study show that the total pore volume was higher in PC mortar than in AACM mortar. Nevertheless, a higher capillary pore volume was observed in AACMs while their gel pore volume was much lower than PC mortar. For example, AACM 1 and 2 mortar has higher percentage of capillary pore volume of 4.04% and 5.69% respectively compared with 3.19% for the control PC mortar under wet/dry curing (Table 4, Figures 11, 12 and 13). On the other hand, the percentage of gel pore volume of 0.60% and 0.98% in AACM 1 and 2 respectively was much lower than 10.83% for PC mortar under wet/dry curing. A similar trend is observed under wet and dry curing (Table 4, Figures 11, 12 and 13).

3.3.4 Strength-porosity relationship of AACM mortars

Strength and porosity data of AACM mixes 1, 2, 1a and 2a (Table 1) are considered in this section together with the data for similar AACM mixes which were prepared with other activator dilutions under 4%. The same mix proportions and test procedures outlined in the paper were used for these mixes. The strength-porosity relationship of all the AACM mortars under wet/dry, wet and dry curing together with the combined plot of wet/dry and dry curing is shown in Figure 15. The best fit lines provide a non-linear plot according to the following relationship proposed for porous materials by *Balshin* [35]

$$6 = 6_0(100\% - P)^n \qquad 2$$

Where 6 = Compressive strength, 6_0 = Compressive strength of fully dense material at 0% porosity, P = Porosity and n = Constant.

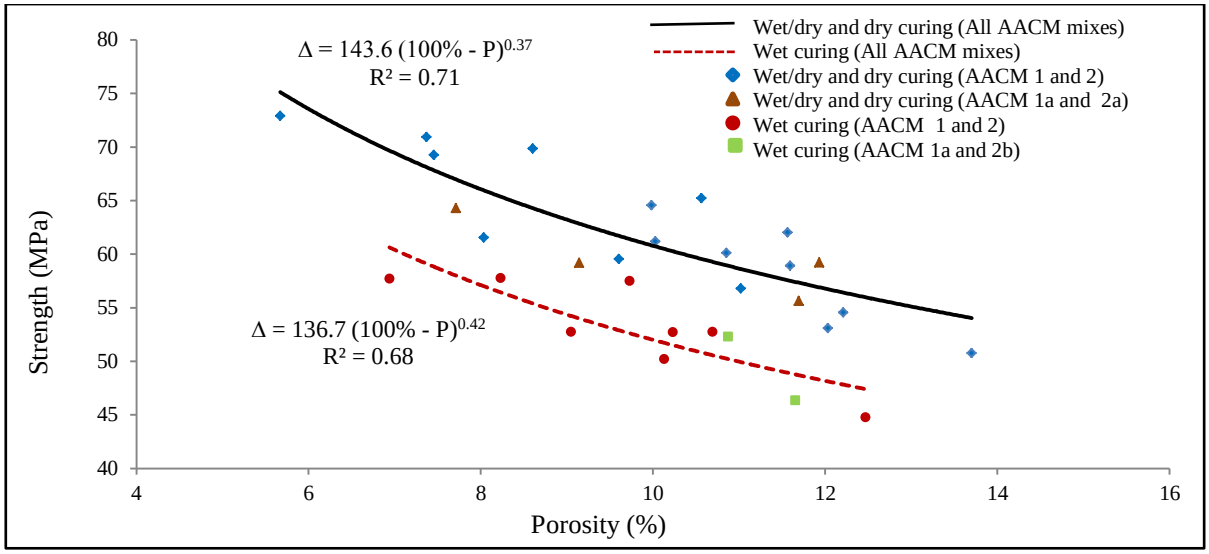

Figure 15: Strength- porosity relationship of AACM mortars under different curing.

A non-linear regression analysis of the data in Fig. 15 using equation 2 provided the following best-fit equation for the combined wet/dry and dry cured AACM mixes.

$$6 = 143.6(100\% - P)^{0.37} \qquad 3$$

With a coefficient of correlation, $R^2 = 0.71$

The corresponding relationship for the wet cured AACM mortars is given by the following equation:

$$6 = 136.7(100\% - P)^{0.42} \qquad 4$$

With a coefficient of correlation, $R^2 = 0.68$

AACM mortar subjected to wet/dry curing had the lowest porosity and highest strength. The initial wet curing aided the production of more geopolymerisation while the subsequent dry curing resulted in increased compressive strength [11]. AACM mortar subjected to wet/dry and dry curing had a higher strength than wet curing in the same range of porosity as shown in Fig. 15. For example from the best-fit relationships, the compressive strength at a porosity

of 10% is 61.2 MPa and 52.7 MPa under wet/dry and wet curing respectively. This indicates an additional effect to porosity which enhances the strength of dry cured AACMs. This can be due to enhanced strength of the geopolymerisation products with dry curing, including increased bond within the geopolymer structure. The initial wet curing also favours the hydration reactions of any high calcium compounds in the AACM binders. Therefore, the optimum curing for strength-porosity relationship in AACMs is achieved under wet/dry curing.

4.0 Conclusions

The paper presents an investigation on the effect of wet, wet/dry and dry curing on the pore size distribution, porosity and strength of an alkali activated cementitious (AACM) mortar and a comparative PC mortar. The AACM mixes were made with and without admixtures (SRA and R42). The following conclusions can be drawn from the results of the study:

1) The wet/dry curing regime produces the highest compressive strength in AACM mortars while it is wet curing for the control OPC mortar. For example, the 28 day strength of AACM 1 mix under wet/dry, wet and dry curing was 70.9MPa, 57.9MPa and 61.2MPa respectively while it was 65.2 MPa, 46.4MPa and 54.6MPa for AACM 2. The corresponding values of 43.4 MPa, 51.4 MPa and 42.3 MPa were observed for OPC mortar.
2) AACM mortar develops a bimodal micropore distribution which is influenced by the type of curing and the activator dilution. Wet/dry curing (3 days in water followed by 24 days in air) provides an optimum pore structure for AACM. OPC mortar develops a unimodal pore structure which is optimum under wet curing.
3) Higher activator concentration, within the range used, results in improved strength and a more refined pore structure. For example, the strength of AACM mortar under wet/dry curing with 0% activator dilution (AACM 1) is 70.9MPa compared

with 65.2MPa for AACM mortar with 7.76% activator dilution (AACM 2). Their corresponding porosity is 4.64% and 6.67%.

4) Wet/dry curing of AACM mortar produces the lowest porosity and pore volume. The porosity of AACM mixes is much lower than the control OPC mortar for each curing condition. For example, AACM 1 mix under wet/dry, wet and dry curing had a porosity of 4.64%, 6.53% and 9.90% respectively. In comparison, the control OPC mortar under wet/dry, wet and dry curing had a porosity of 14.02%, 13.30% and 17.43% respectively, giving the lowest porosity under wet curing.

5) The threshold pore diameters of AACM mixes, which influence durability properties, are at least an order of magnitude lower than for the control OPC mixes. For example, the threshold diameters for AACM 1 mortar under wet/dry, wet and dry curing are 0.013 μm, 0.014 μm, and 0.025 μm respectively. The corresponding values for the control OPC mortar are 0.35 μm, 0.28 μm, and 1.12 μm.

6) The volume of gel pores, within the range of 0.005 μm to 0.01 μm, in AACM mortars is less than the control OPC mortar. On the other hand, the volume of capillary pores, within the range of 0.01 μm to 100 μm pore diameter, is higher in AACM mortars. However, the total porosity (summation of both gel and capillary pores) is higher in the control OPC mortar than in AACM mortars. For example, the gel porosity in AACM 1 and OPC mortar is 0.60% and 10.83% respectively while their corresponding capillary porosity is 4.04% and 3.19% under wet/dry curing.

7) The inclusion of a shrinkage reducing and retarding admixture in AACMs enhances strength and produces a more refined pore structure particularly under wet/dry and dry curing. AACM mortars, both with and without admixtures, have

superior strength and a more refined pore structure than the control OPC mortar under wet/dry and dry curing.

8) The strength-porosity relationship of AACM mortars under combined wet/dry and dry curing is as follows: $6 = 143.6(100\% - P)^{0.37}$ with a coefficient of correlation $R^2 = 0.71$. The relationship under wet curing is given by: $6 = 136.7(100\% - P)^{0.42}$ with $R^2 = 0.68$. For any given porosity, the strength is lower under wet curing.

Acknowledgments

The authors gratefully acknowledge the support of the Materials and Engineering Research Institute, Sheffield Hallam University and the funding provided to the second author for postgraduate study by the Tertiary Education Trust Fund, Ministry of Education, Federal Republic of Nigeria. The authors also acknowledge the recent award by the UK - India Newton - Bhabha programme through funding provided by Innovate UK, EPSRC (EP/P026206/1) and the Government of India for research on AACMs.

References

[1] P.C. Aïtcin, Cements of yesterday and today - concrete of tomorrow, Cem. Concr. Res. 30 (2000) 1349–1359. doi:10.1016/S0008-8846(00)00365-3.

[2] John L. Provis, J.S.J. van Deventer, Alkali-Activated Materials State-of-the-Art Report, RILEM TC 224-AAM, 2014.

[3] N.A. Madlool, R. Saidur, M.S. Hossain, N.A. Rahim, A critical review on energy use and savings in the cement industries, Renew. Sustain. Energy Rev. 15 (2011) 2042–2060. doi:10.1016/j.rser.2011.01.005.

[4] P. Mangat, P. Lambert, Sustainability of alkali-activated cementitious materials and geopolymers, in: Sustain. Constr. Mater., Elsevier Ltd, 2016: pp. 459–476. doi:10.1016/B978-0-08-100370-1.00018-4.

[5] A.M. Neville, Properties of Concrete, Pearson Education Limited, 2011.

[6] R. Kumar, B. Bhattacharjee, Assessment of permeation quality of concrete through mercury intrusion porosimetry, Cem. Concr. Res. 34 (2004) 321–328. doi:10.1016/j.cemconres.2003.08.013.

[7] K.D. Stanish, R.D. Hooton, M.D.A. Thomas, Testing the Chloride Penetration Resistance of Concrete: A Literature Review, 1997.

[8] J.A. Larbi, Microstructure of the interfacial zone around aggregate particles in concrete, Heron. 39 (1993) 1–69.

[9] D. Mindess, Sidney; Young, J. Francis; Darwin, Concrete, Prentice Hall, Pearson Education, Inc. Upper Saddle River, NJ 07458, U.S.A., 2003.

[10] Y. Li, J. Li, Capillary tension theory for prediction of early autogenous shrinkage of self-consolidating concrete, Constr. Build. Mater. 53 (2014) 511–516. doi:10.1016/j.conbuildmat.2013.12.010.

[11] J.C. Petermann, A. Saeed, M.I. Hammons, Alkali-activated geopolymers: a literature review air force research laboratory materials and manufacturing directorate, 2010.

[12] T. Medina-Serna, S. Arredondo-Rea, J. Gómez-Soberón, C. Rosas-Casarez, R. Corral-Higuera, Effect of curing temperature in the alkali-activated blast-furnace slag paste and their structural influence of porosity, Adv. Sci. Technol. Res. J. 10 (2016) 74–79. doi:10.12913/22998624/64021.

[13] G. Fang, W.K. Ho, W. Tu, M. Zhang, Workability and mechanical properties of alkali-activated fly ash-slag concrete cured at ambient temperature, Constr. Build. Mater. 172 (2018) 476–487. doi:10.1016/j.conbuildmat.2018.04.008.

[14] A. Cwirzen, R. Engblom, J. Punkki, K. Habermehl-Cwirzen, Effects of curing: comparison of optimised alkali-activated PC-FA-BFS and PC concretes, Mag. Concr. Res. 66 (2014) 315–323. doi:10.1680/macr.13.00231.

[15] Olalekan.O. Ojedokun and Pal. S. Mangat, Chloride Diffusion in Alkali Activated Concrete, in: II Int. Conf. Concr. Sustain., 2016: pp. 521–531.

[16] BS ISO 15901-1:2016 - Evaluation of pore size distribution and porosity of solid materials by mercury porosimetry and gas adsorption. Mercury porosimetry, 2016.

[17] BS EN196-1, Methods of testing cement - Part 1: Determination of strength, Eur. Stand. (2005) 1–33. doi:10.1111/j.1748-720X.1990.tb01123.x.

[18] BS EN 12350-5 Testing fresh concrete - Part 5: Flow Table Test, Eur. Stand. (2009). doi:10.1007/s13398-014-0173-7.2.

[19] H. Jansson, D. Bernin, K. Ramser, Silicate species of water glass and insights for alkali-activated green cement, AIP Adv. 5 (2015) 67167. doi:10.1063/1.4923371.

[20] V. Sathish Kumar, N. Ganesan, P. V Indira, Effect of Molarity of Sodium Hydroxide and Curing Method on the Compressive Strength of Ternary Blend Geopolymer Concrete, IOP Conf. Ser. Earth Environ. Sci. 80 (2017) 12011. doi:10.1088/1755-1315/80/1/012011.

[21] BS EN 12390-3:2009 Testing Hardened Concrete Part 3: Compressive Strength of Test Specimens, 2009.

[22] BS EN 12390-7:2009, Testing hardened concrete. Density of hardened concrete – BSI British Standards, in: n.d. https://shop.bsigroup.com/ProductDetail/?pid=000000000030164912 (accessed June 21, 2018).

[23] N. Hearn, R.D. Hooton, Sample mass and dimension effects on mercury intrusion porosimetry results, Cem. Concr. Res. 22 (1992) 970–980. doi:10.1016/0008-8846(92)90121-B.

[24] M.M. Reda Taha, A.S. El-Dieb, N.G. Shrive, Sorptivity: a reliable measurement for surface absorption of masonry brick units, Mater. Struct. Constr. 34 (2001) 438–445.

[25] M.I. Mousa, M.G. Mahdy, A.H. Abdel-Reheem, A.Z. Yehia, Self-curing concrete types; water retention and durability, Alexandria Eng. J. 54 (2015) 565–575. doi:10.1016/J.AEJ.2015.03.027.

[26] K. Tan, O.E. Gjorv, Performance of concrete under different curing conditions, Cem. Concr. Res. 26 (1996) 355–361.

[27] D. Khale, R. Chaudhary, Mechanism of geopolymerization and factors influencing its development: A review, J. Mater. Sci. 42 (2007) 729–746. doi:10.1007/s10853-006-0401-4.

[28] A.C. Garrabrants, F. Sanchez, D.S. Kosson, Leaching model for a cement mortar exposed to intermittent wetting and drying, AIChE J. 49 (2003) 1317–1333. doi:10.1002/aic.690490523.

[29] K.K. ALIGIZAKI, Pore structure of cement-based materials: testing, interpretation and

627 requirements, Taylor & Francis, Abingdon [England], 2006.
628 [30] H. Ma, Mercury intrusion porosimetry in concrete technology: Tips in measurement, pore
629 structure parameter acquisition and application, J. Porous Mater. 21 (2014) 207–215.
630 doi:10.1007/s10934-013-9765-4.
631 [31] T.C. Powers, A discussion of cement hydration in relation to the curing of concrete, Highw.
632 Res. Board Proc. 27 (1948). https://trid.trb.org/view.aspx?id=102345 (accessed June 29,
633 2017).
634 [32] R.G. Patel, D.C. Killoh, L.J. Parrott, W.A. Gutteridge, Influence of curing at different relative
635 humidities upon compound reactions and porosity in Portland cement paste, Mater. Struct. 21
636 (1988) 192–197. doi:10.1007/bf02473055.
637 [33] A.T.C. Guimarães, G. De Vera, F.T. Rodrigues, C. Antõn, M.A. Climent, Comparison
638 between Dcrit Considering the Abrupt Variation and Inflexion in the Concrete Mercury
639 Intrusion Porosimetry Curve, Exp. Tech. (2015). doi:10.1111/ext.12002.
640 [34] J.M. Khatib, P.S. Mangat, Porosity of cement paste cured at 45C as a function of location
641 relative to casting position, Cem. Concr. Compos. 25 (2003) 97–108. doi:10.1016/S0958-
642 9465(01)00093-2.
643 [35] Balshin M.Y., Relation of Mechanical Properties of Powder Metals and their Porosity and the
644 Ultimate Properties of Porous-Metal Ceramic Materials, 67 (1949) 831–834.